J Mater Sci (2008) 43:4675–4683
DOI 10.1007/s10853-008-2487-3

REACTIVITY OF SOLIDS

A mechanism of nucleation during thermal decomposition of solids

Loïc Favergeon · Michèle Pijolat · Céline Helbert

Received: 14 September 2007 / Accepted: 18 January 2008 / Published online: 30 April 2008

Abstract A microscopic model based on the appearance, diffusion, and aggregation of point defects allows to calculate the time of appearance of the first nucleus on a surface during a reaction between a solid and a gas. Calculated distributions of these times of appearance of the first nucleus are qualitatively compared to experimental ones, previously determined. The appearance of the point defects seems to be the most influential step on the time of appearance of the first nucleus. Moreover the comparison between experimental and calculated distributions allows to conclude that the frequency of appearance of the defects is higher on the edges than on the faces of the single crystal.

Introduction

Two different processes occur during the reactions of a solid's decomposition, and more generally during the reactions between a solid and a gas: nucleation and the growth of nuclei.

Nucleation is the process responsible for the appearance of the nuclei, which are the smallest possible volume of the new solid phase. Then the growth of these nuclei corresponds to the development of the new solid phase, to the detriment of the initial solid phase.

This growth process is quite well understood for reactions between a solid and a gas [1–4]. On the contrary, the nucleation process remains much less well known, and it is notably very difficult to find quantitative data about this process in the literature.

Numerous questions remain unanswered concerning the nucleation mechanism during solid/gas reactions, especially about the size of the nucleus, its shape, the precise mechanism for the nucleus formation, etc.

In order to try to answer some of these questions, we decided to study the model reaction of the dehydration of lithium sulfate monohydrate single crystals, which has been studied extensively [5–18]. This reaction corresponds to the equation:

$$Li_2SO_4 \cdot H_2O(s) \rightarrow Li_2SO_4(s) + H_2O(g). \quad (1)$$

The progress of the reaction as a function of time was followed by isothermal thermogravimetry at a constant pressure of water vapor. The kinetic curves of conversion versus time, $\alpha(t)$, could be explained due to a nucleation and isotropic growth model for α varying from 0 to 1 [14–16]. We observed that induction periods were systematically present at the beginning of the dehydration of each single crystal, so we focused our study on the modeling of the initial part of the $\alpha(t)$ curves. It was shown that it is possible to calculate, for each single crystal, the experimental time of appearance of the first nucleus from the experimental kinetic curve. These works provide evidence that the distributions of the experimental times of appearance of the first nucleus depend on the water vapor pressure. Indeed, these distributions are shifted towards longer times when the water vapor pressure increases. Moreover their shape presents one mode at low water

---

L. Favergeon (✉) · M. Pijolat
LPMG CNRS UMR 5148 Centre SPIN, Ecole Nationale Supérieure des Mines, 158 Cours Fauriel, 42023 Saint-Etienne Cedex 02, France
e-mail: favergeon@emse.fr

C. Helbert
Département 3MI, Ecole Nationale Supérieure des Mines, 158 Cours Fauriel, 42023 Saint-Etienne Cedex 02, France

vapor pressure, and two modes when the water vapor pressure increases. The first mode seems to be due to the nucleation on the single crystal's edges, whereas the second one seems to be due to nucleation on the single crystal's faces.

In order to explain these phenomena, we decided to describe the nucleation process by means of a microscopic model based on the appearance, diffusion, and aggregation of precursors, which are elementary defects.

The aim of this model of nucleation is to reproduce as accurately as possible the process of nucleation and to determine the time of appearance of the first nucleus at a surface in given conditions.

Description of the model

The mathematical details of the model are given elsewhere [19]. In this paper, we just present the general structure of the modeling, the results obtained for the dehydration of the $Li_2SO_4 \cdot H_2O$ surface, and their comparison to experiments.

The symbols, their signification, and their units used in the following text are summarized in Table 1.

The model consists of a microscopic and probabilistic approach in two dimensions, and requires a discretization of both space and time.

The modeling is based on static aspects, which represent the physical reality, and dynamic aspects to account for the induction time.

The static aspects are the following:

- the single crystal is a three-dimensional lattice; the arrangement of atoms and molecules corresponds to the crystallographic structure of the solid,
- locally, the surface of the single crystal is an ordered plane of atoms and molecules, it is a two-dimensional structure,
- the nucleus is a part of the crystallographic plane of the surface, this part being sufficiently disturbed to allow the change of chemical phase. The element which disturbs the lattice is called a defect. In general, it corresponds to the addition (or the removal) of a molecule or an atom to (or from) one particular site of the lattice. The nucleus is then characterized by a geometry (a set of lattice nets) and a composition (the number of defects necessary for the phase change).

The model is also based on two dynamic aspects:

- The creation of the defects occurs randomly: the defects are formed at random in space (in the crystallographic structure) and in time. From a probabilistic point of view, the appearance of the defects is modeled by a discrete Poisson process, using a parameter χ that represents the average number of new defects created by unit of time and by unit of area. The probability that a defect appears in a surface site during the time interval $[t,t+dt]$ is equal to $1 - \exp(-s_0\chi dt)$, where s_0 is the area of an elementary site.
- Once appeared, the defect can move at the surface and can migrate to a neighbor site. This migration is all the easier as the defect is then in a lower-energy state. The resulting configuration of the atoms is thus more stable. This phenomenon of migration also occurs at random: each defect has several neighbors, what makes several sites of reception possible.

During the time interval $[(k-1)\Delta t, k\Delta t]$, the ability that a defect has to move depends on one hand on the intrinsic mobility of the particles (diffusion aspect) in the structure, which is parameterized by the set of parameters $\alpha_1,\ldots,\alpha_v$ (v being the number of neighbors) and on the other hand on the attraction of the defects: to each possible configuration after migration corresponds an energy that quantifies its attractive capability. For a binary image X (1 being a defect present on site j, and 0 not) at N sites, the energy is equal to:

$$H(X) = \sum_{i=1}^{N} \sum_{j=i_1}^{i_v} \left(X^i - X^j\right)^2. \qquad (2)$$

Table 1 List of symbols used in the model

Symbol	Signification	Unit
s_0	Surface of an elementary site	m^2 or $Å^2$
χ	Frequency of appearance of water vacancies	Number of vacancies m^{-2} unit of time^{-1}
β	Coefficient of attraction of the water vacancies	None
α_i	Intrinsic mobility of the water vacancies in the i direction	None
d_i	Distance between two sites in the i direction	m^2 or $Å^2$
$P_\beta(X)$	Potential corresponding to a surface configuration	None
p_j	Probability	None
D	Diffusion coefficient of the water vacancies	m^2 unit of time^{-1}

To this energy is associated a potential which is equal to $P_\beta(X) = \exp(-\beta H(X))$. This potential is stronger when the image is homogeneous, i.e., the defects are grouped.

Thus, the probability that a defect from image X moves to form an image I_i is than equal to:

$$p_j = \frac{\alpha_j P_\beta(I^{i_j})}{\sum_{l=1}^{v} \alpha_l P_\beta(I^{i_l}) + \left(1 - \sum_{l=1}^{v} \alpha_l\right) P_\beta(X)}. \qquad (3)$$

This probability is proportional to the potential of the image coming from the migration. Thus, the migration supports the regrouping of the defects.

The defects migration law depends on the parameters $\alpha_1,\ldots,\alpha_v$ and β. The parameters $\alpha_1,\ldots,\alpha_v$ depend on the temperature. Indeed, the intrinsic mobility of the defects in the structure is easier when the temperature is high. According to [20, 21], the parameter α_i is linked to the average diffusion coefficient D of the defect by the relation:

$$D\Delta t = \sum_i \alpha_i d_i^2.$$

The appearance of a nucleus is then the consequence of the dynamic of this process, and more precisely of the coalescence of defects, which results from their appearance and their migration at the surface.

The time is discretized arbitrarily. Nevertheless the choice of the time step is such that the processes of appearance and migration of defects are elementary processes between two successive instants.

Results and discussion

For this model of nucleation, five parameters determine the model of nucleation:

- the size and the shape of the surface's tiling,
- the frequency of appearance of water vacancies, denoted by χ,
- the parameter of attraction of vacancies, denoted by β, and
- the diffusion coefficient of the vacancies, denoted by D.

In order to determine the shape and the size of the network, we refer to a previous work [22]. In this work, we carried out some microscopic investigations of both the bulk and surface of $Li_2SO_4{\cdot}H_2O$ by means of atomistic simulations. We noted that the most stable surface of a $Li_2SO_4{\cdot}H_2O$ single crystal is the (−1 0 1) face. As a consequence, we chose this face to determine the shape and size of the surface tiling for lithium sulfate monohydrate. We used a rectangle, with dimensions equal to 4,860 × 8,305 Å^2 and containing two lithium atoms, one sulfate group, and one water molecule. This rectangle allows the entire surface to be recovered by simple translations.

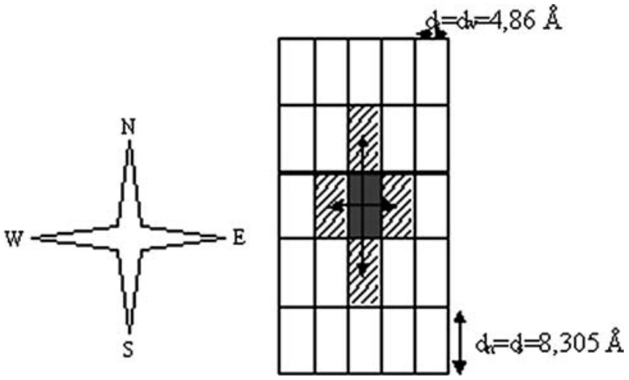

Fig. 1 Tiling used to represent the (−1, 0, 1) face of $Li_2SO_4{\cdot}H_2O$

Thus we retain that an elementary site has a surface $s_0 = 40{,}362$ Å^2 and that distances between neighbor sites are $d_e = d_o = 4{,}860$ Å in the east–west direction and $d_n = d_s = 8{,}305$ Å in the north-south direction, as indicated in Fig. 1.

This choice of a rectangular tiling allows us to simplify the relation between the parameters α_i and the average diffusion coefficient of the defect. Each site having four neighbors, Eq. 4 becomes:

$$D\Delta t = \alpha_n d_n^2 + \alpha_e d_e^2 + \alpha_s d_s^2 + \alpha_w d_w^2. \qquad (5)$$

Moreover, as $d_n = d_s$ and $d_e = d_w$, the probability of migration of a defect from one site to its east neighbor is the same as that for migration to its west neighbor. This equality also holds for the north and south direction, what means:

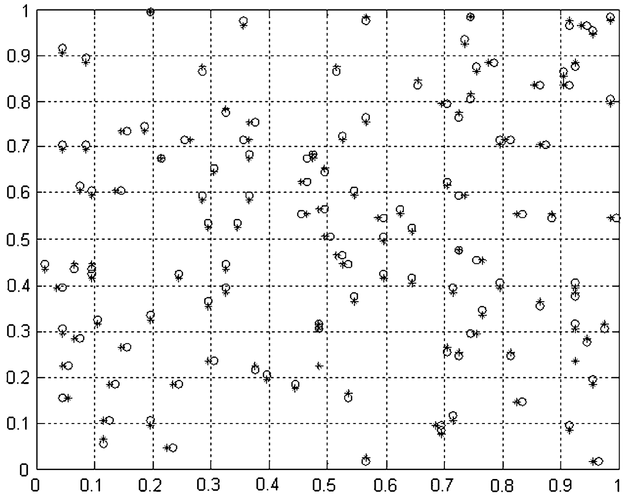

Fig. 2 Snapshot of a surface at two instants t and $t + \Delta t$. The circles represent the positions of the defects at time t and the crosses represent the defects at time $t + \Delta t$

$$\alpha_n = \alpha_s \text{ and } \alpha_e = \alpha_w \quad (6)$$

So Eq. 5 becomes:

$$\frac{D\Delta t}{2} = \alpha_n d_n^2 + \alpha_e d_e^2. \quad (7)$$

In order to simplify the calculations, and in consideration of both paths (east–west and north–south), we decided that the probability of migration is twice as easy in the east or west directions than in the north or south ones, so $\alpha = \alpha_e = 2\alpha_n$.

So, in the case of lithium sulfate monohydrate, the relation (7) between the average coefficient of migration and the parameter α becomes:

$$\alpha = \frac{D\Delta t}{2\left(d_n^2 + 4d_e^2\right)}.$$

Except for the size and shape of the surface tiling, it has not been possible to determine the other parameters in the experimental conditions of our study (a temperature of 80°C and a water vapor pressure in the range 2.6–4.6 hPa). Indeed, the energy required to remove a single water molecule has been determined only at 0 K and under vacuum. The determination of the diffusion coefficient of the water vacancies requires a complete study using molecular dynamics, which has not been done yet.

For our simulations, we decided to use the following values:

- the frequency of appearance of the defects χ is in the range 10^{14}–10^{15} defects by unit of time,
- the parameters of attraction β is between 0 and 1,

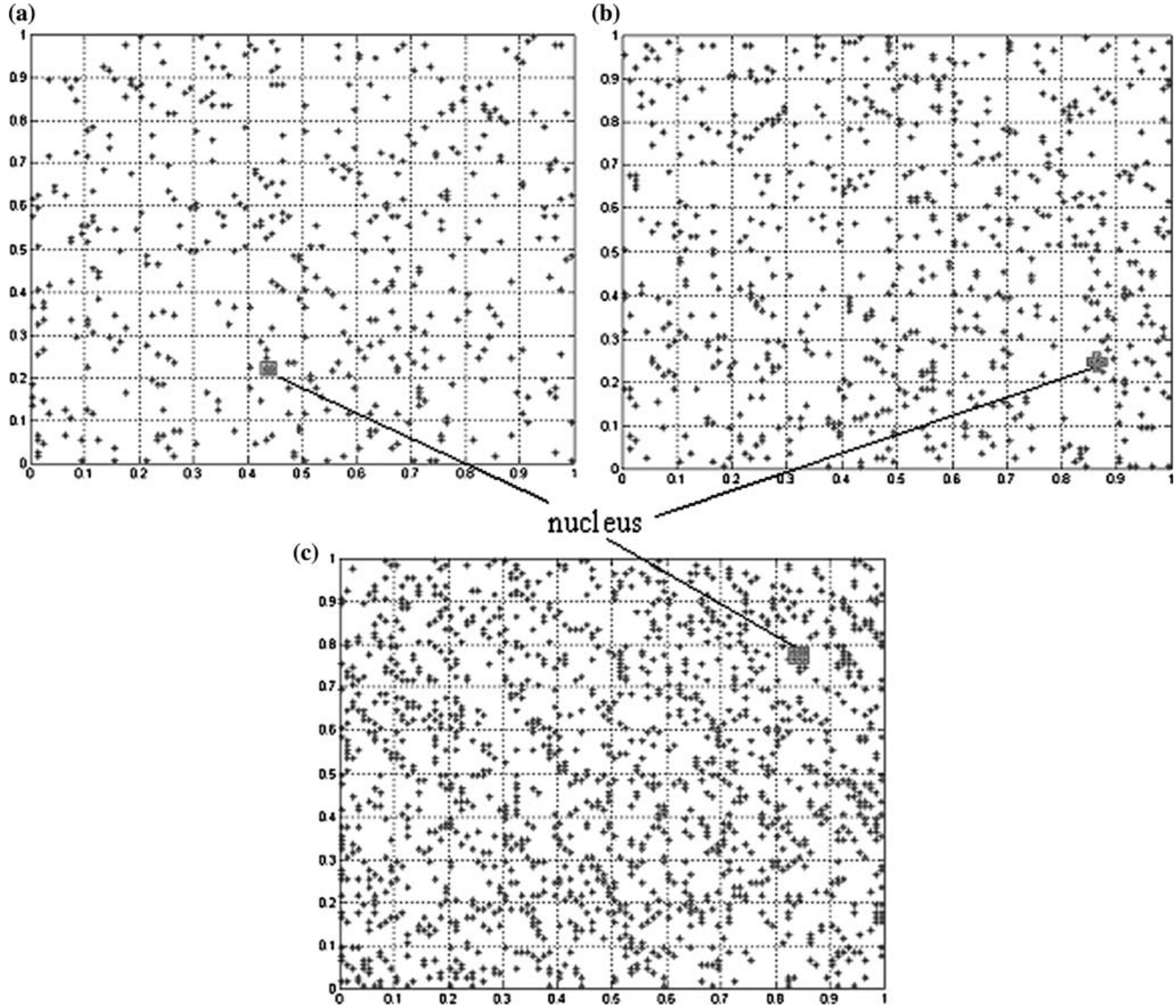

Fig. 3 Snapshot of surfaces at the time of appearance of the nucleus for three different configuration of the nucleus: (**a**) nucleus formed by four defects with square shape, (**b**) nucleus formed by five defects with cross shape, and (**c**) nucleus formed by nine defects with square shape

- the diffusion coefficient of the defect D is in the range 10^{-19}–10^{-21} m^2 unit of time^{-1}

At each time t, defects can appear. Between two instants t and $t + \Delta t$, defects can migrate in the four directions (north, south, east, and west) or not migrate. Figure 2 represents a snapshot of a surface at two different instants t and $t + \Delta t$. In this figure, the parameters of the simulation are: 100 × 100 sites, $\Delta t = 1$, $\chi = 10^{15}$, $D = 10^{-19}$, and $\beta = 0.4$.

The shape and the size of a nucleus (i.e., the number of defects which formed this nucleus) are chosen arbitrarily. Figure 3 represents the surface when the first nucleus appears, for three different configurations of the nucleus (four defects with square shape, five defects with cross shape, and nine defects with square shape). For these simulations the parameters were as follow: 100 × 100 sites $\Delta t = 1$, $\chi = 10^{15}$, $D = 10^{-19}$, and $\beta = 0.4$.

Moreover, the model allows to consider a defect initially present at the surface of the solid. For the moment, only one defect can be positioned, which represents 0.1‰ of the surface sites (for 100 × 100 sites). This defect is fixed on the surface during all the simulation time. It can represent a water vacancy existing before the beginning of the reaction, a surface defect or even a single crystal edge. Figure 4 represents two surfaces with an initial defect fixed at the coordinates (3,3)—the indexed origin being situated in the bottom left corner—at the instant of appearance of the nucleus formed by nine defects with a square shape. The nucleus is not necessarily formed where the initial defect is (Fig. 4b). Nevertheless, we note that, even when the nucleus is not formed where the initial defect is placed, this zone gathers a lot of defects. For these figures the simulation parameters were 100 × 100 sites, $\Delta t = 1$, $\chi = 10^{15}$, $D = 10^{-19}$, and $\beta = 0.4$.

For a given set of parameters (shape and size of the nucleus, χ, D, β), we can perform an important number of simulations in order to obtain as many times of appearance of the first nucleus. Thus we can calculate distributions of the times of appearance of the first nucleus.

The following results were obtained with 50 simulations (we have verified that the shape of the distributions are identical to those obtained with 200 simulations).

By changing one parameter (the others being constant), we can see the influence of each of them on the distributions.

The distributions represented in Fig. 5 show that, the higher the number of defects that form the nucleus, the longer the time necessary to form the nucleus, as expected. One can also note that the shape of the nucleus is not very importance: both distributions obtained with a nucleus formed by two defects (horizontal or vertical) are roughly the same.

Figure 6 represents the influence of three parameters: the frequency of appearance of the defects, the defect mobility, and the attraction parameter. For each parameter, three different values are used: a low, an intermediate, and a high value. These distributions allow the observation that the frequency of appearance of the defects is the most influential parameter on the time of appearance of the first nucleus; the attraction coefficient and the defects mobility have less impact. Figure 6a, in particular, suggests that, for a given single crystal, if two distinct frequencies of

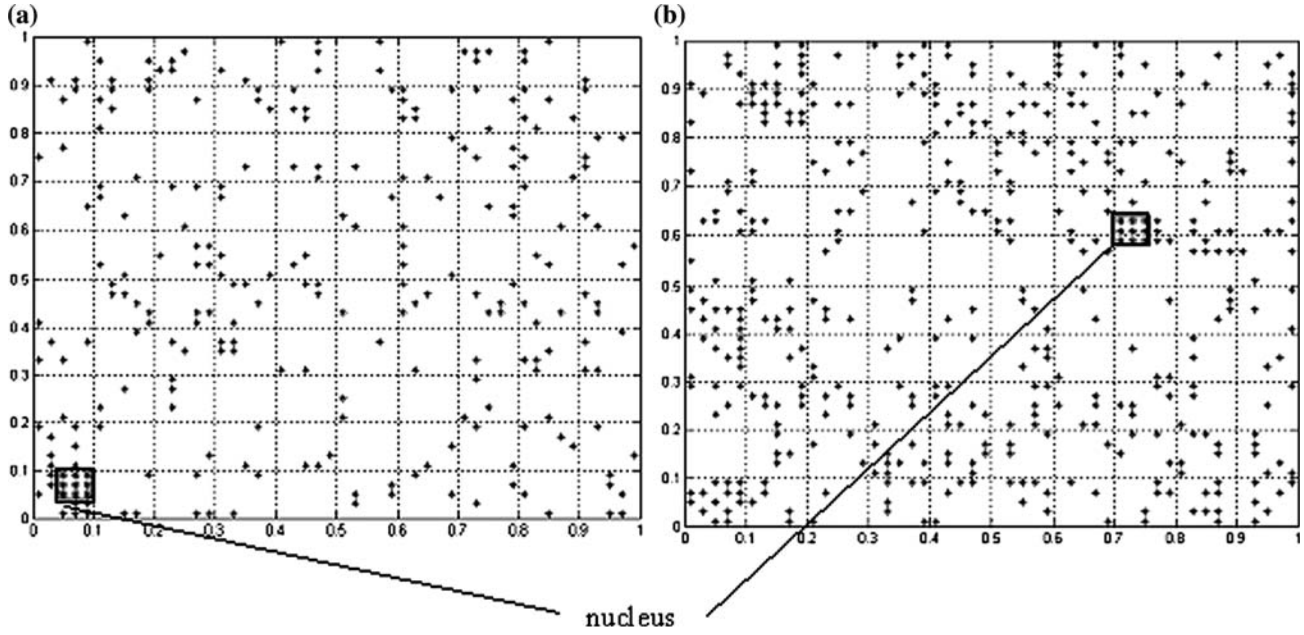

Fig. 4 Snapshot of surfaces at the time of appearance of the nucleus with an initial defect at the coordinates (3,3): (**a**) the nucleus appeared near this defect and (**b**) the nucleus appeared elsewhere

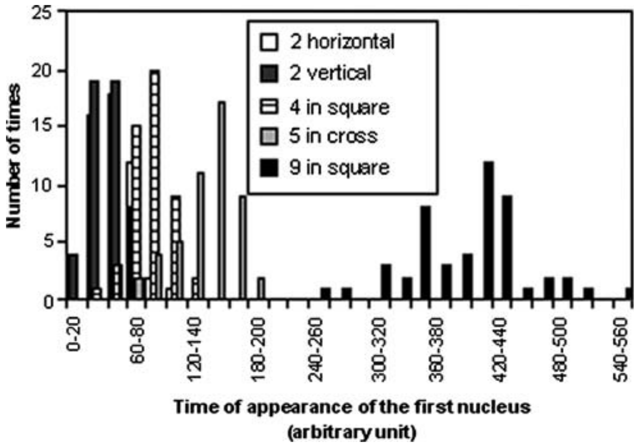

Fig. 5 Distributions of 50 times of appearance of the first nucleus: influence of the number of defects and of the nucleus shape, the other parameters being: 100 × 100 sites, $\Delta t = 1$, $\chi = 10^{15}$, $D = 10^{-19}$, and $\beta = 0.4$

appearance of the defects coexist on the same surface, the distribution should be bimodal.

For the case of the presence of an initial defect at the surface (located at coordinates (3,3)), the results are presented in Fig. 7 for the influence of the size and the shape of the nucleus, and in Fig. 8 for the influence of the others parameters (frequency of appearance of the defects, defect mobility, and defect attraction).

The presence of an initial defect does not change the influence of the parameters on the time of appearance of the first nucleus: a nine-defect square still forms more slowly than a four-defect square, and the frequency of appearance of the defects is still the most influent parameter.

It is also possible to compare the distributions obtained with the same parameters, with and without an initial defect as shown in Fig. 9.

This figure shows that the presence of an initial defect appreciably decreases the time of appearance of the first

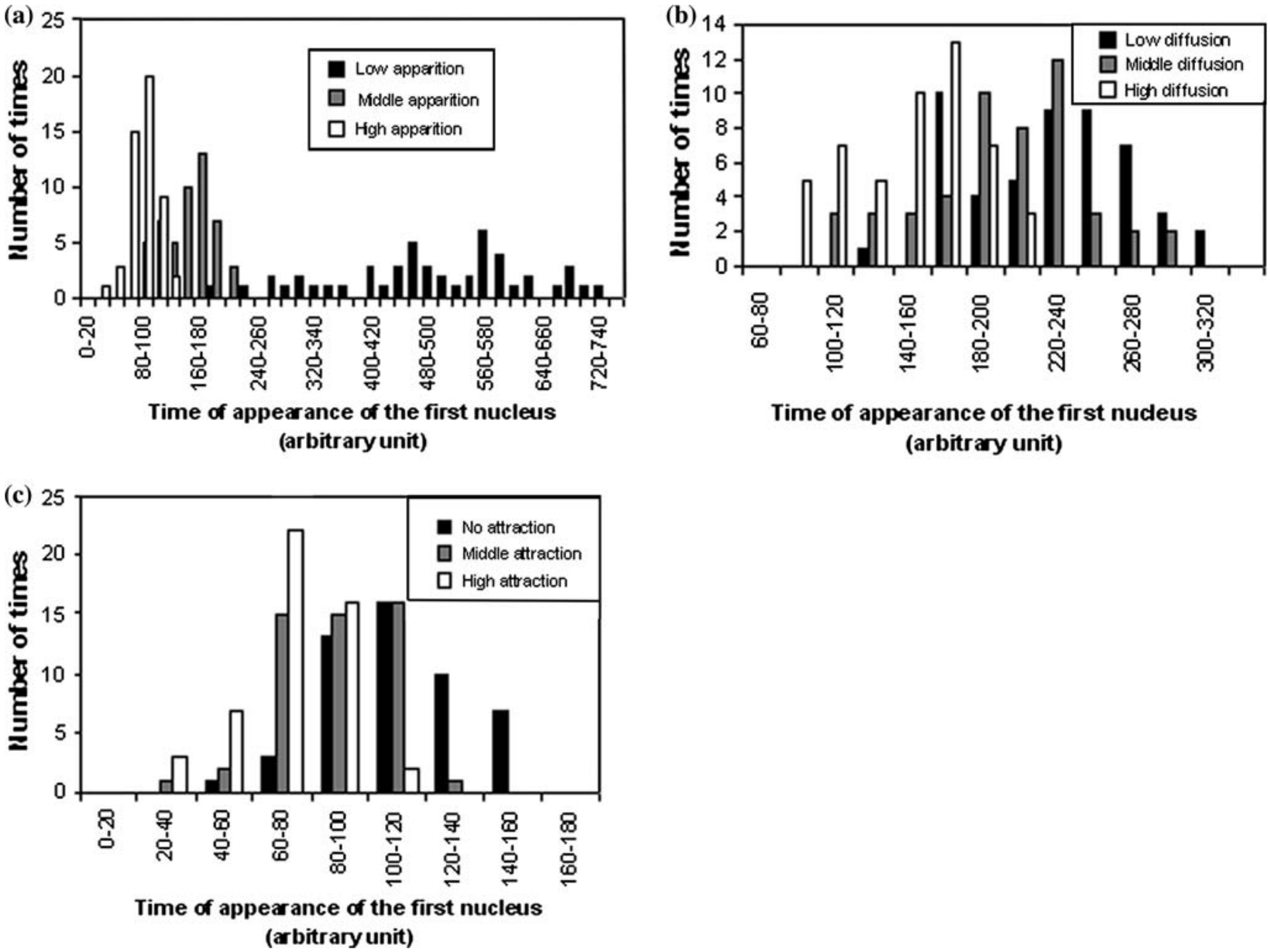

Fig. 6 Distributions of 50 times of appearance of the first nucleus: influence (**a**) of the frequency of appearance of the defects, (**b**) of the defect mobility, and (**c**) of the attraction parameter

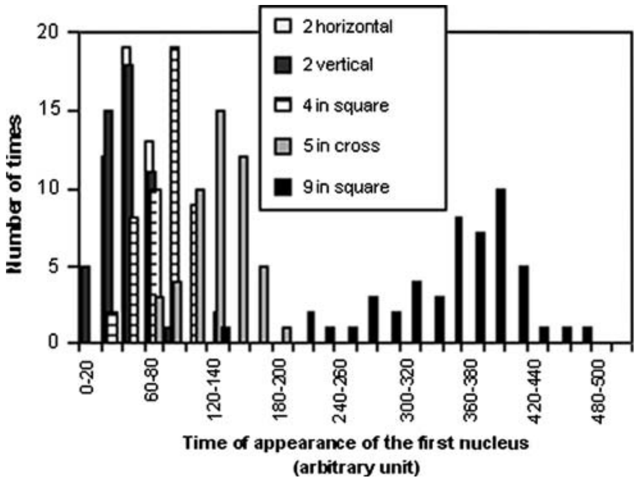

Fig. 7 Distributions of 50 times of appearance of the first nucleus with the presence of an initial defect: influence of the number of defects and of the nucleus shape

nucleus, whatever the shape of the nucleus. It is highly probable that increasing the number of these defects would reduce the times (for the simulations presented on Fig. 9, there is one initial defect for 10,000 sites).

Now we can compare experimental distributions of the times of appearance of the first nucleus obtained in a previous work [18] mentioned in the Introduction, with distributions calculated by using the described model of nucleation.

The surface element area being $s_0 = 40{,}362$ Å^2 and the lithium sulfate monohydrate single-crystal surface being in the range 5–10 × 10^{-5} m^2, a complete representation of a single crystal's surface requires roughly 10^{14} sites, what is too large a number for simulation. So we will limit ourselves to simulations on a 100 × 100 sites and to qualitative interpretations. Moreover all the parameters of the model have not yet been determined in the experimental conditions (which are 80°C with a water vapor pressure in the range 2.6–4.6 hPa).

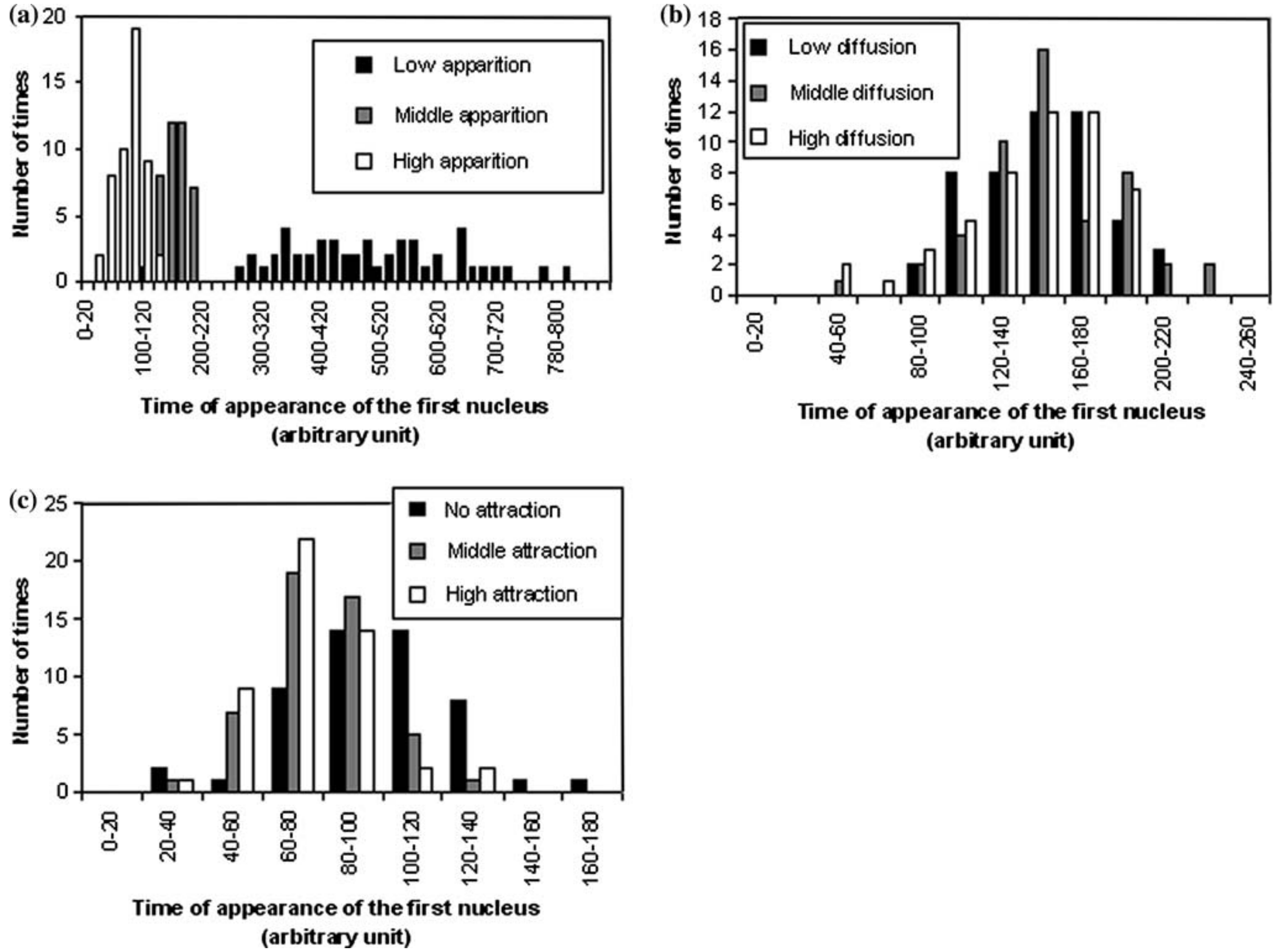

Fig. 8 Distributions of 50 of appearance of the first nucleus with the presence of an initial defect: influence (**a**) of the frequency of appearance of the defects, (**b**) of the defect mobility, and (**c**) of the attraction parameter

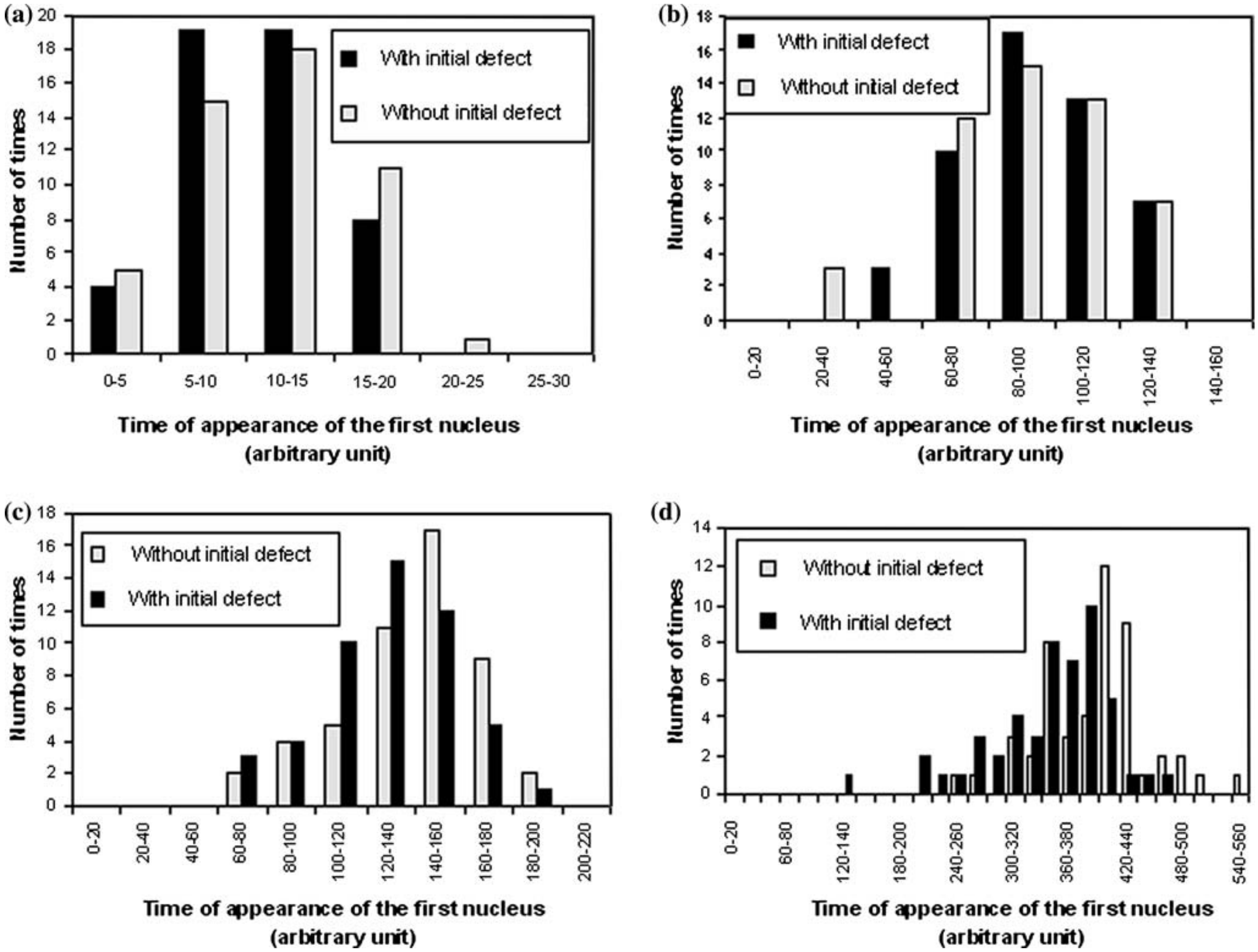

Fig. 9 Distributions of 50 times of appearance of the first nucleus with and without an initial defect: (**a**) vertical nucleus with two defects, (**b**) square nucleus with four defects, (**c**) cross nucleus with five defects, and (**d**) square nucleus with nine defects

Experimental distributions of the times of appearance of the first nucleus indicate that induction periods are greater and that distributions are spread over a larger range when the water vapor pressure is increased. For the calculated distributions, a decrease in the frequency of appearance of the defects has exactly the same impact. This is expected if one considers that the defect is a vacancy of water molecule, since their concentration is expected to decrease with an increase in water vapor pressure.

Moreover, we have seen that, when the water vapor pressure is increased, the distribution of the times of appearance of the first nucleus becomes bimodal. Nevertheless, whatever the parameter of the simulation we vary, it is not possible to obtain bimodal calculated distributions. However the existence of two different frequencies of appearance of defects results in a bimodal distribution, as shown in Fig. 10. Using environmental scanning electron microscopy, we have seen in [17] that one mode (the fastest) can be attributed to nucleation on the edges and the other mode (the slowest) to nucleation on the faces, so we can attribute one of these frequencies of appearance of defects to the faces of the single crystal and the other to their edges. This implies that the frequency of appearance of defects is higher on the edges than on the faces of the single crystals. Even if the simulations from the nucleation model give qualitative trends, it is worth noting that they reproduce the experimental data very well.

Conclusion

A microscopic model was used in order to determine the time of appearance of the first nucleus at a surface during a reaction between a solid and a gas. This model is based on the appearance and aggregation of precursors, these precursors being point defects such as water vacancies in the case of dehydration.

A parametric study of the model determined that the frequency of appearance of the defects is the most

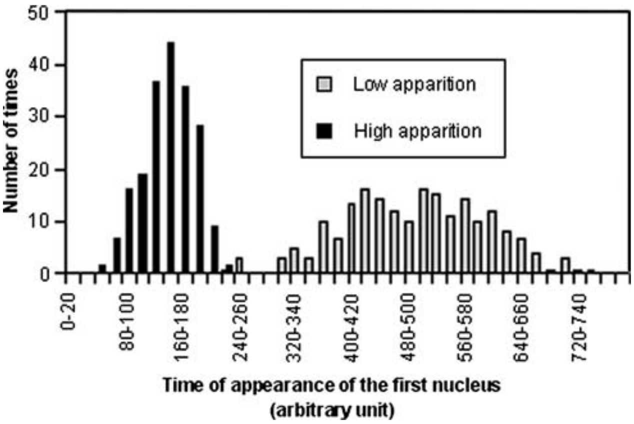

Fig. 10 Example of the distribution of the times of appearance of the first nucleus using two different frequencies of appearance of defects (obtained with 2 × 200 simulations)

influential parameters on the time of appearance of the first nucleus.

Moreover, a qualitative comparison with experimental results allows an explanation for the existence of two modes of nucleation to be proposed and to conclude that the frequency of appearance of the defects is higher on the edges than on the faces of the single crystals.

Acknowledgement The authors wish to thank Françoise Valdivieso for her contribution to this work.

References

1. Jacobs PWM, Tompkins FC (1955) In: Garner WE (ed) Chemistry of the solid state, chap 7. Butterworths, London
2. Brown ME, Dollimore D, Galwey AK (1980) In: Bamford CH, Tipper CFH (eds) Reactions in the solid state, Comprehensive chemical kinetics, vol 22. Elsevier, Amsterdam
3. Jacobs PWM (1997) J Phys Chem B 101:10086
4. Galwey AK, Brown ME (1999) Thermal decomposition of ionic solids. Elsevier, Amsterdam
5. Okhotnikov VB, Yakobson BI, Lyakhov NZ (1983) React Kinet Catal Lett 23:125
6. Okhotnikov VB, Simakova NA, Kidyarov BI (1989) React Kinet Catal Lett 39:345
7. Kirdyashkina NA, Okhotnikov VB (1988) React Kinet Catal Lett 36:417
8. Gaponov YA, Kidyarov BI, Kirdyashkina NA, Lyakhov NZ, Okhotnikov VB (1988) J Therm Anal 33:547
9. Koga N, Tanaka H (1989) J Phys Chem 93:7793
10. Galwey AK, Koga N, Tanaka H (1990) J Chem Soc Faraday Trans 86:531
11. Brown ME, Galwey AK, Li Wan Po A (1992) Thermochim Acta 203:221
12. Valdivieso F, Bouineau V, Pijolat M, Soustelle M (1997) Solid State Ionics 101–103:1299
13. Modestov AN, Poplaukhin PV, Lyakhov NZ (2001) J Therm Anal 65:121
14. Favergeon L, Pijolat M, Valdivieso F, Helbert C (2005) Phys Chem Chem Phys 7:3723
15. Favergeon L, Valdivieso F, Pijolat M (2006) In: Proceedings NATAS conference, Bowling Green, KY, USA
16. Favergeon L (2006) PhD Thesis, Ecole Nationale Supérieure des Mines, Saint-Étienne
17. Favergeon L, Pijolat M, Thermochimica Acta (submitted)
18. Favergeon L, Pijolat M, Soustelle M, Thermochimica Acta (submitted)
19. Helbert C, PhD thesis, Ecole Nationale Supérieure des Mines, Saint-Étienne, France
20. Guyon E, Hulin JP, Petit L (1991) Hydrodynamique physique. Ed CNRS, Paris
21. Guyon X (1993) Champs aléatoires sur un réseau: modélisations, statistique et applications. Masson, Paris
22. Favergeon L, Valdivieso F, Pijolat M, Fisher CAJ, Islam MS, J Phys Chem C (submitted)